ELSEVIER

Journal of Alloys and Compounds 229 (1995) 134–143

Journal of ALLOYS AND COMPOUNDS

# Crystal chemistry of superconducting copper oxycarbonates

B. Raveau, C. Michel, B. Mercey, J.F. Hamet, M. Hervieu

*Laboratoire CRISMAT, ISMRA et Université de Caen, Boulevard du Maréchal Juin, 14050-Caen Cedex, France*

Received 17 January 1995; in final form 8 March 1995

**Abstract**

The high $T_c$ superconducting oxycarbonates form a large class whose crystal chemistry is presented herein. In the form of bulk materials, five families of oxycarbonates, involving lanthanides, thallium, bismuth, lead and mercury, have been synthesized with $T_c$ values up to 80 K. Laser ablation appears to be a very promising new soft chemistry method to synthesize new oxycarbonates in the form of thin films. This is illustrated by the phases $(CaCuO_2)_m$ and $(Ba_2CuO_2CO_3)_n$, that exhibit $T_c$ values up to 100 K.

*Keywords:* Crystal chemistry; Superconductivity; Copper oxycarbonates

## 1. Introduction

The discovery of superconductivity in copper oxides has meant that the extraordinarily rich chemistry of these perovskite-related systems has been studied in detail (for a review, see Ref. [1]). In addition to the extensive families of lanthanide, bismuth, thallium, lead and mercury cuprates, a large series of copper oxycarbonates has been discovered during the last 3 years. The main characteristic of these phases is the ability of the carbonate groups to replace copper, forming intergrowths of perovskite, rock salt and carbonate layers. A remarkable feature is that many of these compounds exhibit a higher critical temperature than the corresponding cuprates. Moreover, the metastable character of these phases means that particular experimental conditions are sometimes required for their synthesis. In this paper, we report the crystal chemistry and superconducting properties of these new compounds, prepared in the form of bulk materials or stabilized as thin films.

## 2. The bulk superconducting oxycarbonates

Starting from the oxycarbonate $Sr_2CuO_2CO_3$ [2], whose structure (Fig. 1) consists of single perovskite layers interconnected with rows of $CO_3$ groups, a superconductor can be obtained by replacing strontium by barium, with a $T_c$(onset) of 40 K [3,4]. The quantitative synthesis of oxycarbonates requires that they be prepared in evacuated ampoules, starting from adequate mixtures of alkaline earth carbonate, copper and alkaline earth or rare earth oxides, at low temperature in order to avoid explosion. This is the case for the "123" derivatives, $(Y,Ca)_n(Ba,Sr)_{2n}Cu_{3n-1}CO_3O_{7n-3}$, whose structure consists of an ordered replacement of rows of $CuO_4$ groups by $CO_3$ groups.

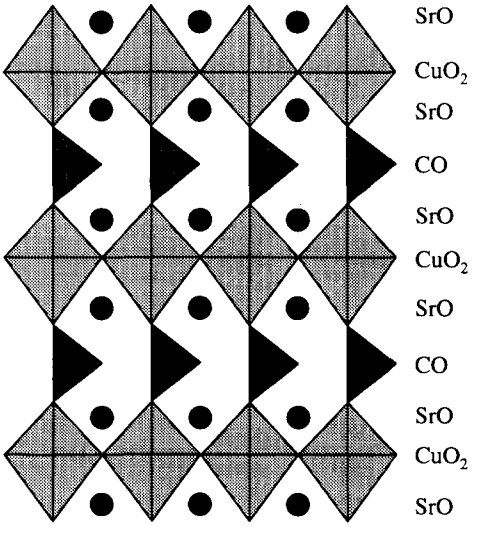


Fig. 1. Schematic representation of the structure of the oxycarbonate $Sr_2CuO_2CO_3$. Triangles represent the carbonate groups.


*SSDI* 0925-8388(95)01679-1

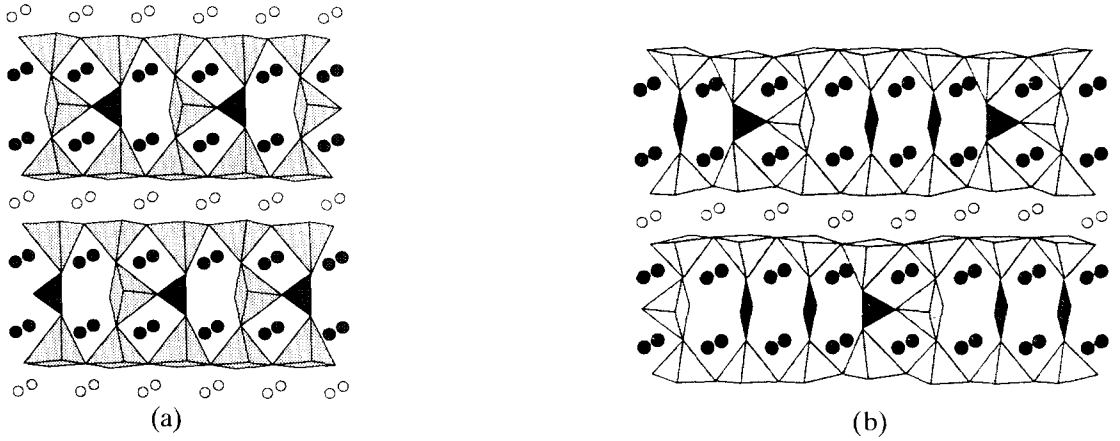

Fig. 2. Structure of the $n = 2$ (a) and $n = 3$ (b) members of the oxycarbonate series $(Y,Ca)_n(Ba,Sr)_{2n}Cu_{3n-1}C_3O_{7n-3}$.

The oxycarbonates $(Y_{1-x}Ca_x)_{0.95}Sr_{2.05}Cu_{2.4}(CO_3)_{0.6}O_y$ [5] and $YCaBa_4Cu_5(NO_3)_{0.3}(CO_3)_{0.7}O_{11}$ [6,7] represent the $n = 2$ members of this series (Fig. 2(a)) with $T_c$(onset) values of 66 and 82 K respectively. Curiously, no superconductivity was observed for the $n = 3$ member $Y_4Sr_8Cu_{11}CO_3O_{25}$ [8] (Fig. 2(b)) and for $Y_{1.6}Ca_{0.4}Ba_4Cu_5CO_3O_{11}$ ($n = 2$) [2].

The bismuth oxycarbonates [10–12] $(Bi_2Sr_2CuO_6)_n(Sr_2CuO_2CO_3)_{n'}$ represent the third family, whose structure (Fig. 3) can be described as an intergrowth of the 2201 structure of $Bi_2Sr_2CuO_6$ [13] with $Sr_2CuO_2CO_3$ [2], i.e. as 2201 layers interconnected through carbonate layers. In fact, only the $n = 1$ members have been synthesized to date. This is the case for the 30 K superconductor $Bi_2Sr_4Cu_2CO_3O_8$ (Fig. 3(a)), the 40 K superconductor $Bi_2Sr_{6-x}Cu_3(CO_3)_2O_{10}$ (Fig. 3(b)) and the 34 K superconductor $Bi_{2-x}Pb_xSr_8Cu_4(CO_3)_3O_{12}$ (Fig. 3(c)). These $n' = 1, 2, 3$ members correspond to the intergrowth of a single 2201-type layer with a single, double and triple $Sr_2CuO_2CO_3$-type layer respectively. It should be noted that their critical temperature is always larger than that of the parent phase $Bi_2Sr_2CuO_6$ (22 K). It is worth pointing out that the synthesis of these phases is delicate: they are prepared in gold foils in air using appropriate thermal treatments [10–12]. In addition to these superconductors, a new oxycarbonate, $Bi_{15}Sr_{29}(CO_3)_7O_{56}$ [14], has been synthesized recently. Although it does not superconduct, this phase is of great interest since it is closely related to the $n = 1$ member. Its structure (Fig. 4) consists of $Bi_2Sr_4Cu_2CO_3O_8$ ribbons that are seven $CuO_6$ octahedra wide; two successive ribbons are shifted with respect to each other across the $(010)_{2201}$ plane, so that the $[CuO_2]$ layers are interrupted. This phase can be considered as a collapsed oxycarbonate, which results from a shearing operation, on every seventh octahedron, in the "$m = 1$, $n = 1$" member of the bismuth oxycarbonate series $(Bi_2Sr_2CuO_6)_m(Sr_2CuO_2CO_3)_n$. The latter mechanism is interesting, since it suggests the possibility of creating columnar defects in high $T_c$ superconductors to improve pinning.

The fourth family of oxycarbonates corresponds to the thallium phases, with the general formula $[(Tl,A)Sr_2CuO_5]_n[(Sr_2CuO_2CO_3)]_{n'}$. The oxycarbonates $Tl_{0.5}A_{0.5}Sr_4Cu_2CO_3O_7$, with A ≡ Pb and Bi [15,16], represent the members "$n = n' = 1$" of this series. The structure of these tetragonal phases (Fig. 5) consists of the intergrowth of double rock salt layers $[(Tl_{0.5}A_{0.5})(SrO)]$ and single perovskite layers, linked through layers of $CO_3$ groups. Both compounds exhibit a sharp transition, with $T_c$ values of 70 K and 54 K respectively. In fact, they can be described as the intergrowth of the two structures $Sr_2CuO_2CO_3$ (Fig. 1) and "1201", i.e. $Tl_{0.5}A_{0.5}Sr_2CuO_5$ with A ≡ Pb and Bi [17–19] (Fig. 6). The remarkable feature of these two compounds is that the two structures which form their framework either do not superconduct or exhibit a lower $T_c$ value. $Sr_2CuO_2CO_3$ has indeed never been observed to superconduct, whereas only traces of superconductivity up to 60 K were detected in the 1201 phase $Tl_{0.5}Pb_{0.5}Sr_2CuO_5$ [18], which might be due to the presence of traces of oxycarbonate. In a similar way, the 1201 cuprate $(Tl,Bi)Sr_2CuO_5$ is characterized by a lower $T_c$ value with a broad transition [19]. Clearly, the intergrowth of two parent structures improves significantly the superconducting properties. The 62 K superconductor $TlSr_{4-x}Ba_xCu_2CO_3O_7$ [20] is closely related to the first two thallium oxycarbonates. It can be obtained from the latter structure by a shearing mechanism (Fig. 7), i.e. by a translation along $c$ every fourth octahedral row, by a $c/2$ vector, so that the $[CuO_2]$ and $[SrO]$ layers of each block remain unchanged and form infinite (001) layers (Fig. 8). This is not the case for the $[TlO]$ ribbons which are limited to four Tl atoms along $b$ and are connected to ribbons of four $CO_3$ groups. Consequently, mixed layers of $[(TlO)_4(CO)_4]$ are obtained involving a sequence of four thallium atoms and four carbonate groups along $b$. This results in a strong waving of the octahedral

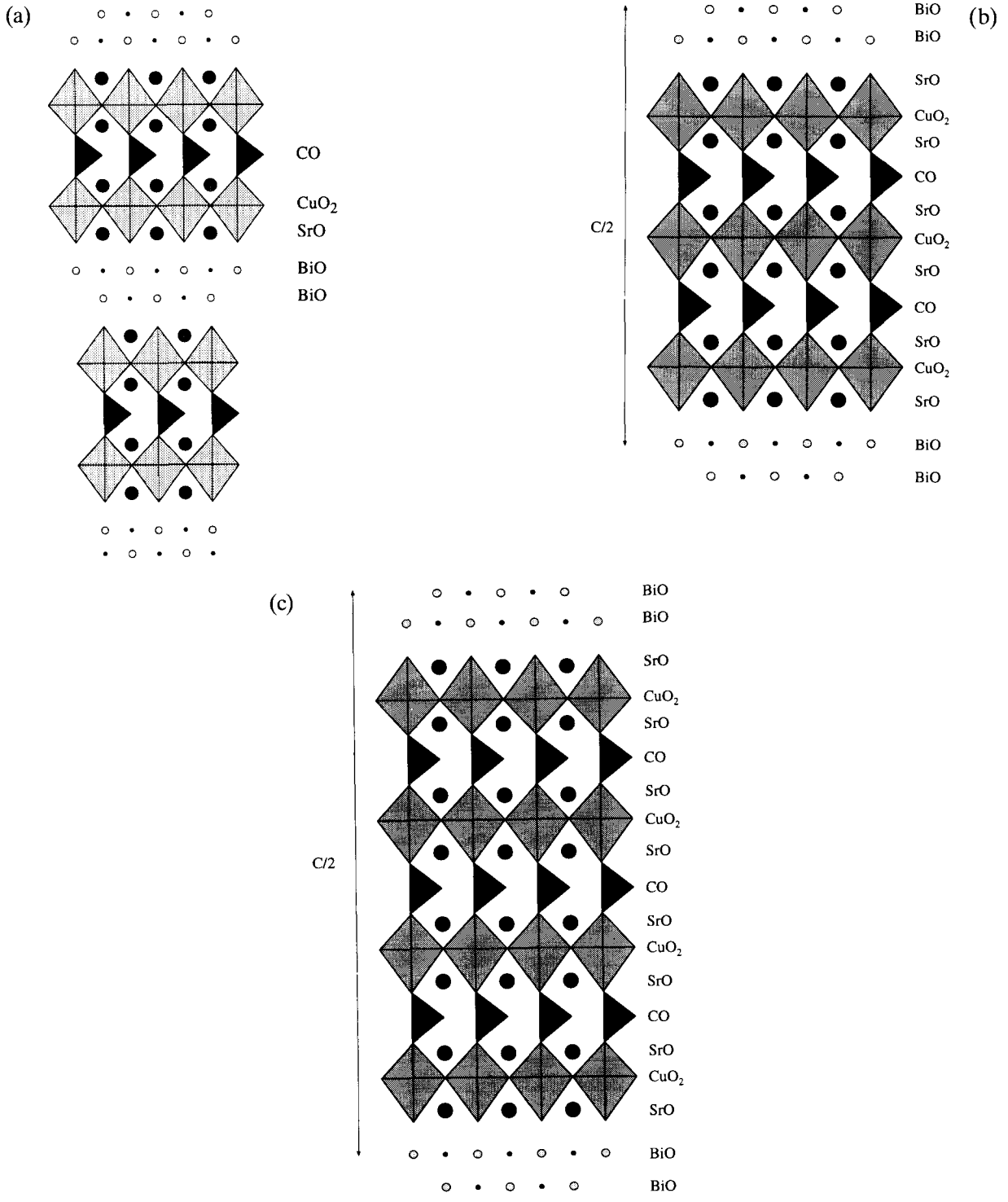


Fig. 3. Structure of the three members of the series $(Bi_2Sr_2CuO_6)_n(Sr_2CuO_2CO_3)_{n'}$: (a) $n = 1$, $n' = 1$; (b) $n = 1$, $n' = 2$; (c) $n = 1$, $n' = 3$.

copper layers (Fig. 8) in order to accommodate the large size difference between thallium and carbon. Thus two successive perovskite layers wave in antiphase so that the larger space between such layers is occupied by thallium, the $CO_3$ groups being located in the narrower spaces. This framework can also be described as a "1201"-type structure in which the [TlO] layers are replaced by ordered mixed $[(TlO)_4(CO)_4]$ layers. We observe again that the critical temperature of this phase is higher than that of the parent structures, since $TlSr_2CuO_5$ [21] does not superconduct, whereas $TlBa_2CuO_5$ [22] and $TlBaSrCuO_5$ [23] exhibit $T_c$ values of 10 K and 43 K respectively.

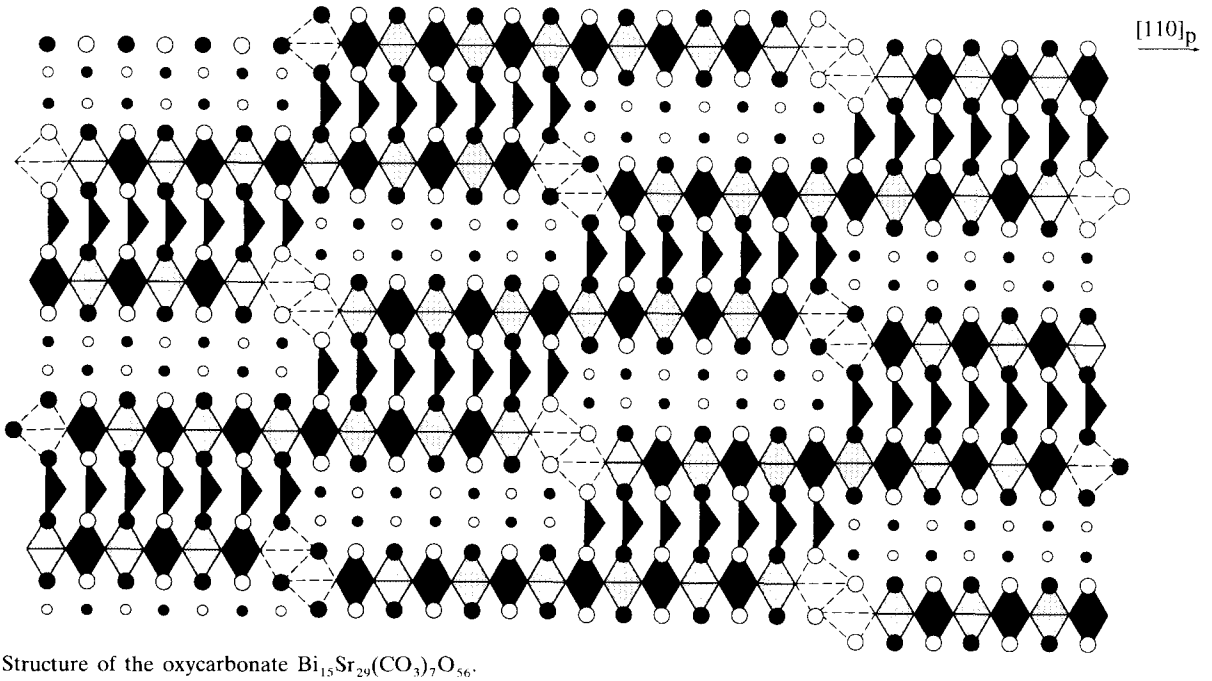


Fig. 4. Structure of the oxycarbonate $Bi_{1.5}Sr_{2.9}(CO_3)_7O_{5.6}$.

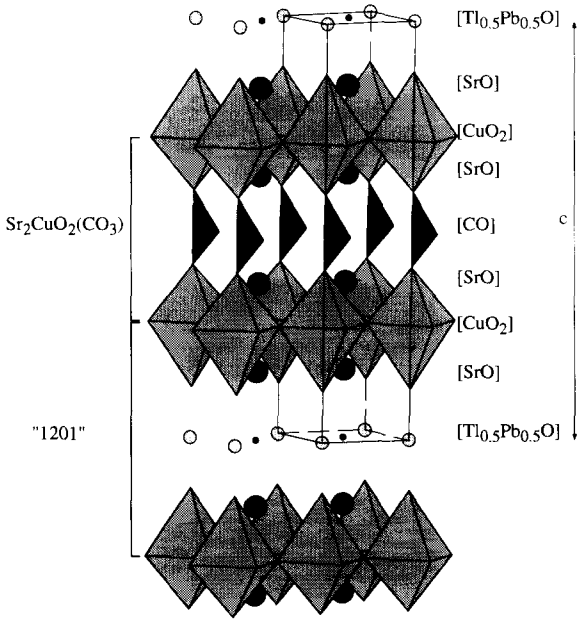


Fig. 5. Structure of the oxycarbonate $Tl_{0.5}A_{0.5}Sr_4Cu_2CO_3O_7$.

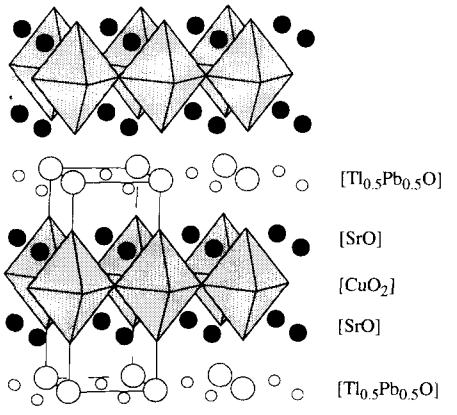


Fig. 6. Structure of the "1201" cuprate $Tl_{0.5}A_{0.5}Sr_2CuO_5$.

Soon after the discovery of superconductivity in $HgBa_2CuO_4$ [24], the possibility to generate mercury oxycarbonates was considered. Three oxycarbonates have been isolated to date; they are all isotypic with the thallium phases. The 70 K superconductor $HgBa_2Sr_2Cu_2CO_3O_7$ [25] is closely related to the collapsed oxycarbonate $TlBa_2Sr_2Cu_2CO_3O_7$ (Fig. 8), but differs from the latter by the nature of the shearing plane which is {110} instead of {100}. The oxycarbonate $Hg_{0.3}Pb_{0.7}Sr_4Cu_2CO_3O_{7-\delta}$ [26] also exhibits a sharp transition, with a $T_c$ value of 70 K. The structure of this compound is similar to that of $Tl_{0.5}Pb_{0.5}Sr_4Cu_2CO_3O_7$ (Fig. 6), lead and mercury being statistically distributed on the same sites as thallium, whereas the $[(Hg,Pb)O_{1-\delta}]$ layer is oxygen deficient, as in mercury cuprates. A similar structure has also been observed for $Bi_{0.5}Hg_{0.5}Sr_4Cu_2CO_3O_{7-\delta}$ [27] which exhibits a much lower $T_c$ value of 17 K. In the latter, electron microscopy shows cationic disordering and shearing phenomena, which may explain the low critical temperature of this phase.

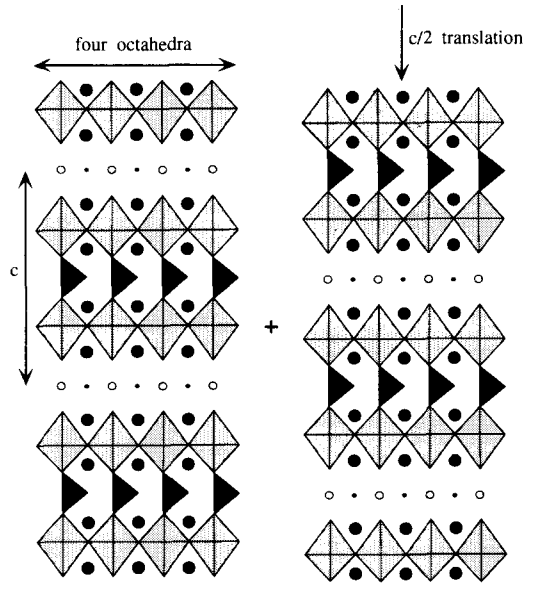


Fig. 7. Illustration of the shearing mechanism leading to the formation of the collapsed oxycarbonate $TlSr_{4-x}Ba_xCu_2CO_3O_7$.

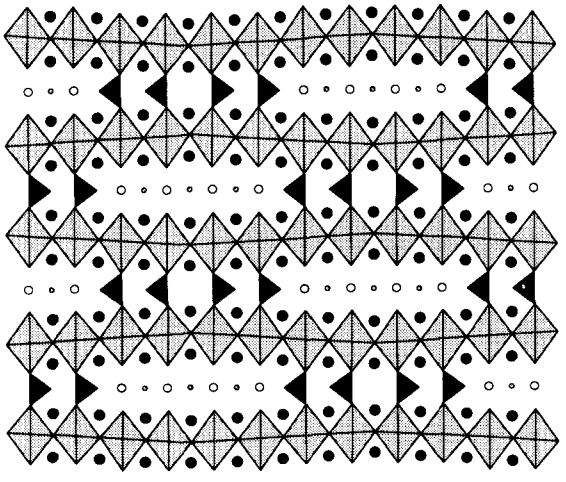

Fig. 8. Structure of the collapsed oxycarbonate $TlSr_{4-x}Ba_xCu_2CO_3O_7$.

## 3. Thin film oxycarbonates: a new series of metastable superconductors $(CaCuO_2)_m(Ba_2CuO_2CO_3)_n$

After the discovery of superconductivity at high temperature in 1987, laser ablation was revealed to be an exceptional tool for depositing thin cuprate films. This method is of considerable interest, since it allows the realization of new metastable frameworks due to the fact that it involves rather low deposition temperatures on the substrate. Thus it can be considered as a new kind of soft chemistry, based on the quasi-epitaxial character of deposition on a monocrystalline substrate.

On the basis of these considerations, the Ba–Ca–Cu–O system was investigated using laser ablation, but introducing various partial pressures of carbon dioxide close to the substrate. Using this method, a new superconducting oxycarbonate family $(CaCuO_2)_m(Ba_2CuO_2CO_3)_n$ was synthesized as thin films [28]. The main phase forming the matrix is $Ba_2Ca_3Cu_4CO_3O_8$ ($m = 3$; $n = 1$).

The films were deposited on the (001) plane of a single crystal $LaAlO_3$ substrate, using a pulsed KrF excimer laser (Lambda Physik) working at $\lambda = 248$ nm. Special preparation of the sintered target was necessary, the best results being obtained for the nominal composition $Ba_2Ca_3Cu_5O_{10}$. The $O_2$ and $CO_2$ pressures were carefully controlled during deposition, the optimization of the film being reached for a gas mixture containing 6% $CO_2$.

The X-ray diffraction (XRD) and electron diffraction (ED) patterns show that this new phase is characterized by a pseudo-cubic subcell characteristic of perovskite and exhibits a tetragonal symmetry with an in-plane $b$ parameter equal to the $a$ parameter perpendicular to the substrate. However, the [001] ED patterns recorded along a direction perpendicular to the substrate plane (Fig. 9) show that the $c$ parameter

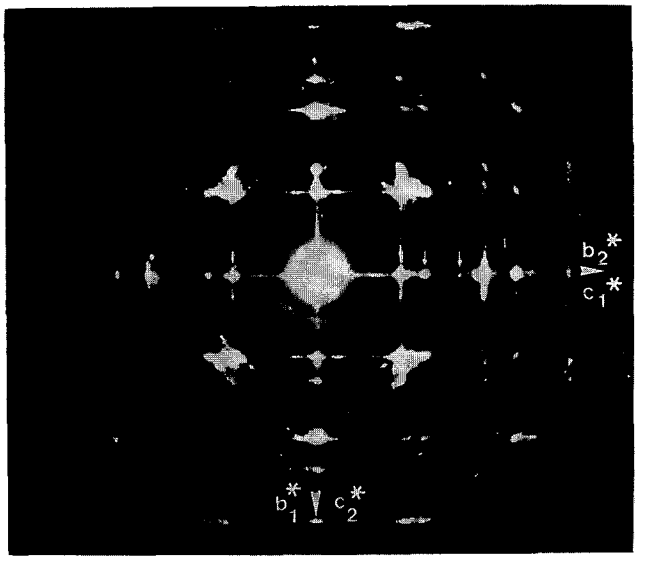


Fig. 9. [100] ED pattern, recorded along a direction perpendicular to the substrate plane. The intense reflections are those of the perovskite subcell. Streaks are observed along the two equivalent directions of the subcell, $c_1^*$ and $c_2^*$. Nodes, indicated by small arrows, are the 006 and 008 reflections of the $m = 4$ member of the series.

in the substrate plane varies, and is a multiple of the subcell $a_p$ parameter ($c \approx (m+2) \times a_p$). Two important structural features are observed. First, streaks are present along two equivalent directions of the perovskite subcell (Fig. 9). Second, from the reconstruction of the reciprocal lattice, it clearly appears that the streaks exist only along one direction, i.e. along $\vec{c}$ (the intense reflections corresponding to the perovskite subcell). Moreover, small nodes are observed which attest that the periodicity along $\vec{c}$ is roughly a multiple of $a_p$, i.e. $c \approx (m+2) \times a_p$. Thus the periodicity along $\vec{c}$, which is supposed to result from an ordering phenomenon, is not well established, so that aleatoric sequences can be expected and the ordering phenomena take place along the two equivalent directions of the subcell, which would involve the formation of 90° oriented domains. These results suggest that the as-grown new tetragonal microphases, with $a \approx a_p$ and $c \approx (m+2) \times a_p$, are $a$ axis oriented with respect to the substrate, i.e. with the $a$ axis perpendicular to the substrate plane.

Energy dispersive spectroscopy (EDS) analyses, performed on several zones of the films, lead to an average cationic composition of the new material (plotted to two for the barium content) of "$Ba_2Ca_{2.9}Cu_{4.15}$". The [100] high- resolution electron microscopy images, recorded for two different focus values (Fig. 10), clearly establish that the contrast is directly related to that observed in the copper-based perovskites and oxycarbonates. In Fig. 10(a), the cation positions are imaged as bright dots ($\Delta f \approx -50$ nm). Such an image allows the sequence of the layers to be identified. The characteristic features of the contrast consist of two rows of very bright dots separated by rows of slightly less bright dots. The very bright dots are correlated with the positions of barium and the less bright dots with the copper positions. Rows of small grey dots are located between the copper layers; they are correlated with the calcium rows. In Fig. 10(b), the zones of light electronic density are imaged as bright dots. It can be seen that, between the rows of dark dots, which are now correlated with

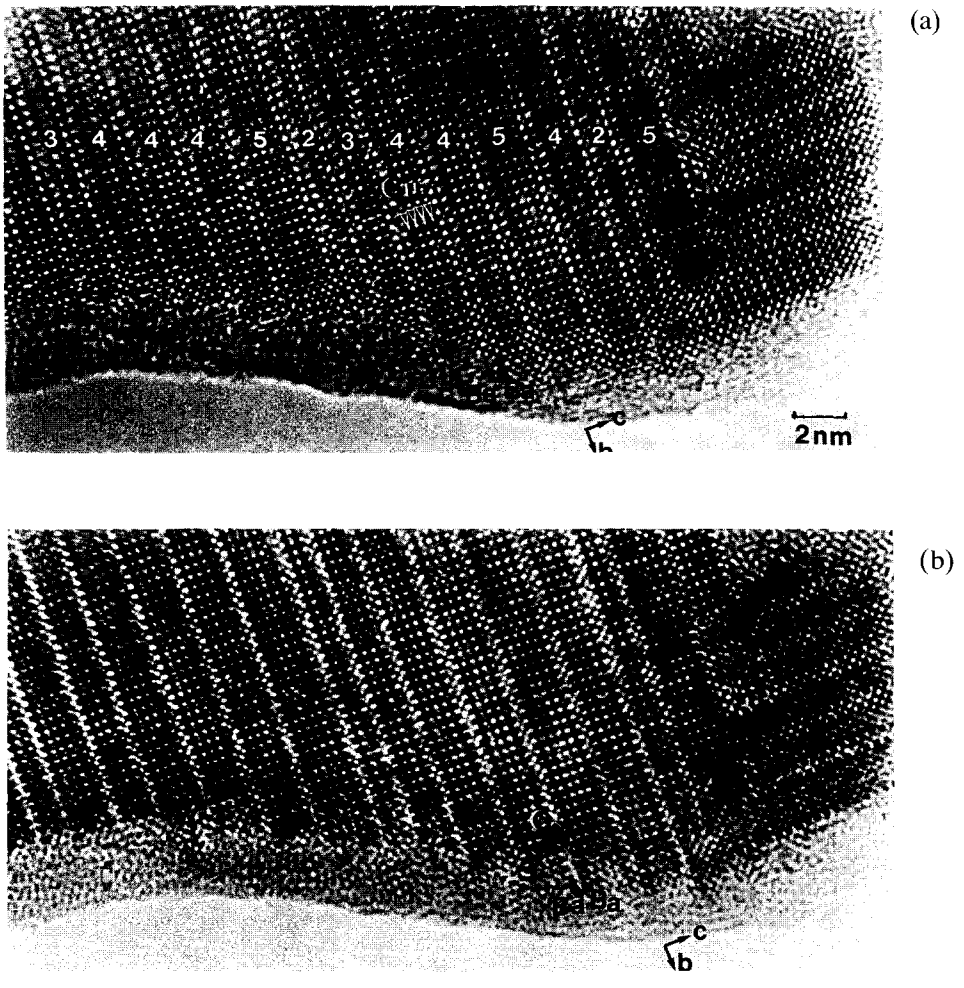


Fig. 10. Enlarged [100] images. (a) The cation positions are imaged as bright dots ($\Delta f \approx -50$ nm); barium and copper layers are identified. The number of copper layers within one slice, i.e. $m+1$, is indicated in the top part of the image. (b) Typical image ($\Delta f \approx -15$ nm) where the carbon rows and surrounding oxygen atoms appear in the form of very bright dots (curved arrow).

the cation positions, there exist two types of rows of bright dots. The first are located between the barium rows and exhibit a contrast which is typical of the rows of carbonate groups, and the second, located between the rows of calcium atoms, are correlated with the copper rows and exhibit a contrast similar to that

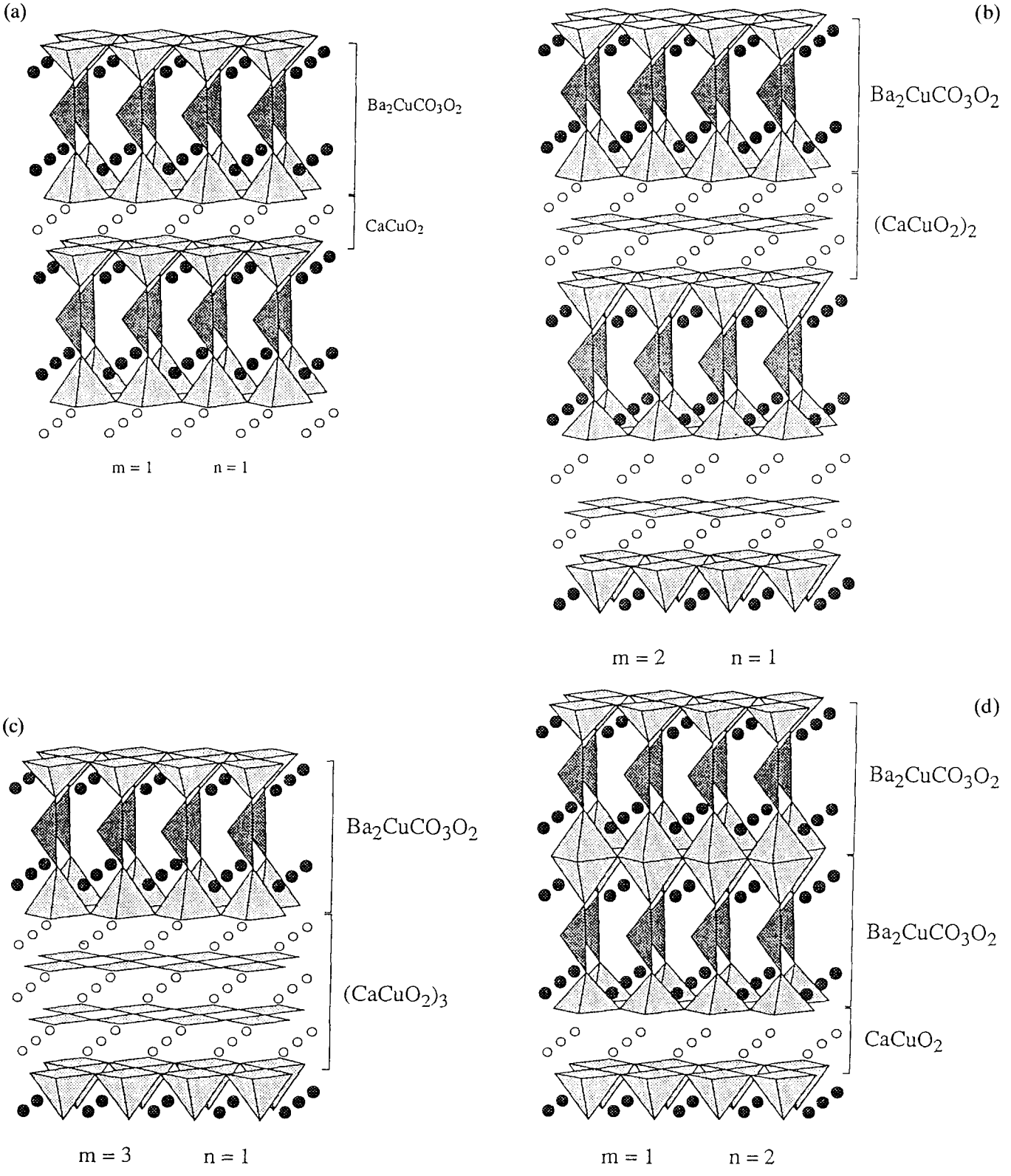


Fig. 11. Idealized structural models of the first members of the family $(CaCuO_2)_m(Ba_2CuO_2CO_3)_n$: (a) $m = 1$, $n = 1$; (b) $m = 2$, $n = 1$; (c) $m = 3$, $n = 1$; (d) $m = 1$, $n = 2$.

observed in 1223 or 1234 cuprates. The interlayer distance between two successive $[CuO_2]_\infty$ layers, close to 3.3 Å, suggests that, in the intermediate copper layers, located between two calcium layers, copper exhibits a square planar coordination, whereas calcium has a cubic coordination.

The number of copper layers between two successive carbonate layers can be easily obtained from these images (see numbers in Fig. 10(a)). It simply corresponds to the number of rows of bright dots intercalated between the two rows of very bright dots. It can be seen that it varies from two to five, but is mainly four. From these observations, a structural model can be proposed which describes the different members of the series (Fig. 11) as derivatives of the infinite layer structure $CaCuO_2$ with intercalated layers of carbonate groups. At the level of each carbonate layer, calcium is replaced by barium, so that one carbonate layer is sandwiched by two BaO layers according to the sequence "$CuO_2$-BaO-CO-BaO- $CuO_2$". Such slices are then stacked with multiple $CaCuO_2$-type layers, so that the general formula of these microphases can be written $(CaCuO_2)_m(Ba_2CuO_2CO_3)_n$. Most of the members observed in this film (Fig. 10(a)) correspond to $n = 1$, whereas $m$ varies in the range 1–4. The structure of the oxycarbonates $(CaCuO_2)_m(Ba_2CuO_2CO_3)_n$ consists of pyramidal copper layers stacked with layers of $CuO_4$ square planar groups and interconnected with layers of carbonate groups, as shown, for example, in the first three members of this series (Figs. 11(a)–11(c)). It should be noted that the $m = 1$ member, $Ba_2CaCu_2CO_3O_4$ (Fig. 11(a)), is directly derived from the "123" structure by replacing rows of $CuO_4$ square planar groups by rows of carbonate groups. The $m = 3$ member, $Ba_2Ca_3Cu_4CO_3O_8$ (Fig. 11(c)), which is the predominantly observed microphase (Fig. 10(a)), consists of quadruple copper layers built up from double $[CuO_2]_\infty$ square planar layers sandwiched between two pyramidal copper layers and interconnected through carbonate layers. The $n > 1$ members are rarely observed; $n = 2$ members appear sometimes as a defect and correspond to the local microphase $CaBa_4Cu_3(CO_3)_2O_6$ ($m = 1$; $n = 2$). The corresponding structural model (Fig. 11(d)) shows that the structure of members $(CaCuO_2)_m(Ba_2CuO_2CO_3)_n$ consists of octahedral and pyramidal copper layers interconnected through layers of carbonate groups. The a.c. susceptibility measurements of the films (Fig. 12) show that the best $T_c$ value is obtained at 6% $CO_2$. The d.c. resistance measurement of a sample grown with a 3% gas composition of $CO_2$ is shown in Fig. 13. The $T_c$ onset is greater than 100 K and zero resistance is reached below 60 K. Above the transition, the signal is noisy, probably owing to the poorly crystallized areas of the film, and the sample shows a semiconducting behaviour.

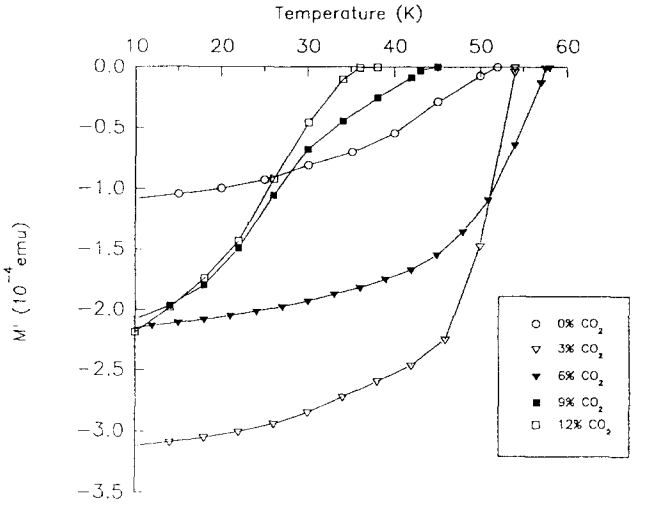


Fig. 12. A.c. magnetic susceptibility measurements of thin films grown at 0%, 3%, 6%, 9% and 12% gas composition of $CO_2$. Dimensions of the film grown under pure oxygen are 3 mm × 2 mm × 1500 Å. Dimensions of the other films are 5 mm × 4 mm × 1500 Å.

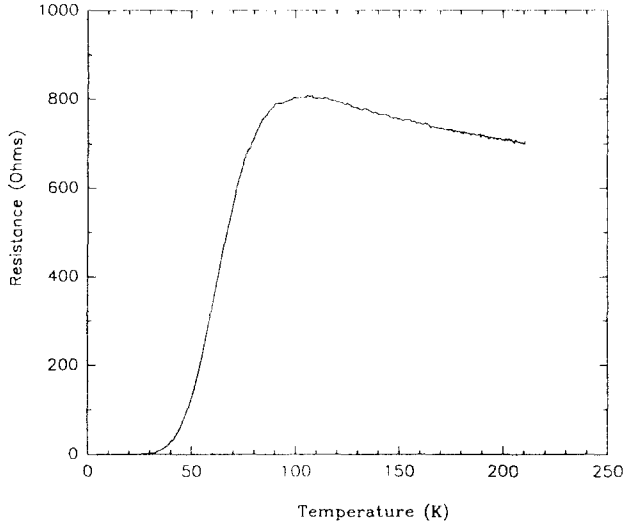


Fig. 13. D.c. resistance measurement of a film grown with a 3% gas composition of $CO_2$.

These new "BaCaCu" oxycarbonates can be compared with those recently synthesized in the form of bulk materials at high pressure [29,30]. Nevertheless, their structure is fundamentally different from those of the high pressure carbonates, such as $(Cu_{0.5}C_{0.5})Ba_2Ca_{n-1}Cu_nO_{2n+3}$ or $Cu_{0.5}C_{0.5}Ba_3Ca_{n-1}Cu_nO_{2n+5}$, by the fact that in the films no "1-1" ordered carbonate/copper layers, i.e. no ordering, has been detected along $b$; thus the copper content of the carbonate layers of these films, if different from zero, can be assumed to be very low. In this respect, the laser ablation method seems to be more effective for

carbonation than the high pressure method since it allows full carbonate layers to be stabilized.

However, the ideal formula of these phases and, particularly, of the main microphase $Ba_2Ca_3Cu_4CO_3O_8$ ($m = 3$; $n = 1$) does not suggest any mixed valent copper, i.e. it implies Cu(II) only, and therefore presents the problem of discovering the origin of the superconductivity in these compounds. The creation of hole carriers necessary for the appearance of superconductivity may result from the fact that $CO_3$ groups are statistically missing in the structure (Fig. 14(a)), inducing mixed valence Cu(II)–Cu(III). Another hypothesis proposes a partial replacement of the $CO_3$ groups by a small number of $CuO_4$ groups (Fig. 14(b)) which would not be seen by high-resolution electron microscopy owing to the statistical distribution of the $CuO_4$ groups over the carbonate positions. EDS analysis, indicating a slight excess of copper with respect to the ideal composition, supports this second hypothesis.

The magnetic and electrical measurements, showing critical temperatures ranging from 30 to 100 K with rather broad transitions, indicate that these materials are at present not optimized, in agreement with the fact that several members are coherently intergrown in the same film. These results open a route to the synthesis of the different members and to the optimization of their superconducting properties by controlling the target composition, the $CO_2/O_2$ atmosphere and the substrate temperature. There is no doubt that it will be possible to isolate thin films of single members, in particular using molecular beam epitaxial laser deposition.

## 4. Conclusions

The copper oxycarbonates form a large series of promising superconducting materials. Their investigation, using special soft chemistry methods, such as laser ablation, should allow new members to be stabilized and optimized in the near future.

## References

[1] B. Raveau, C. Michel, M. Hervieu and D. Groult, *Crystal Chemistry of High $T_c$ Superconducting Cuprates*, Springer Series in Material Sciences 15, Springer, 1991.
[2] D.V. Fomichev, A.L. Kharlanov, E.V. Antipov and L.M. Kovba, *Superconductivity, 3* (1990) 126.
[3] K. Kinoshita and T. Yamada, *Nature, 337* (1992) 312.
[4] F. Izumi, K. Kinoshita, Y. Matsui, K. Yanagisawa, T. Ishigaki, T. Kamiyama, T. Yamada and H. Asano, *Physica C, 196* (1992) 227.
[5] J. Akimitsu, M. Vehara, M. Ogawa, H. Nakata, K. Tomimoto, Y. Miyazaki, H. Yamane, T. Hirai, K. Kinoshita and Y. Matsui, *Physica C, 201* (1992) 320.
[6] A. Maignan, M. Hervieu, C. Michel and B. Raveau, *Physica C, 208* (1993) 116.
[7] M. Hervieu, C. Michel and B. Raveau, *Chem. Mater., 8* (1993) 1126.
[8] B. Domengès, M. Hervieu and B. Raveau, *Physica C, 207* (1993) 65.
[9] M. Hervieu, P. Boullay, B. Domengès, A. Maignan and B. Raveau, *J. Solid State Chem., 105* (1993) 300.
[10] D. Pelloquin, M. Caldès, A. Maignan, C. Michel, M. Hervieu and B. Raveau, *Physica C, 208* (1993) 121.
[11] D. Pelloquin, A. Maignan, M.T. Caldès, M. Hervieu, C. Michel and B. Raveau, *Physica C, 212* (1993) 199.
[12] D. Pelloquin, M. Hervieu, A. Maignan, C. Michel, M.T. Caldès and B. Raveau, *J. Solid State Chem., 112* (1994) 362.

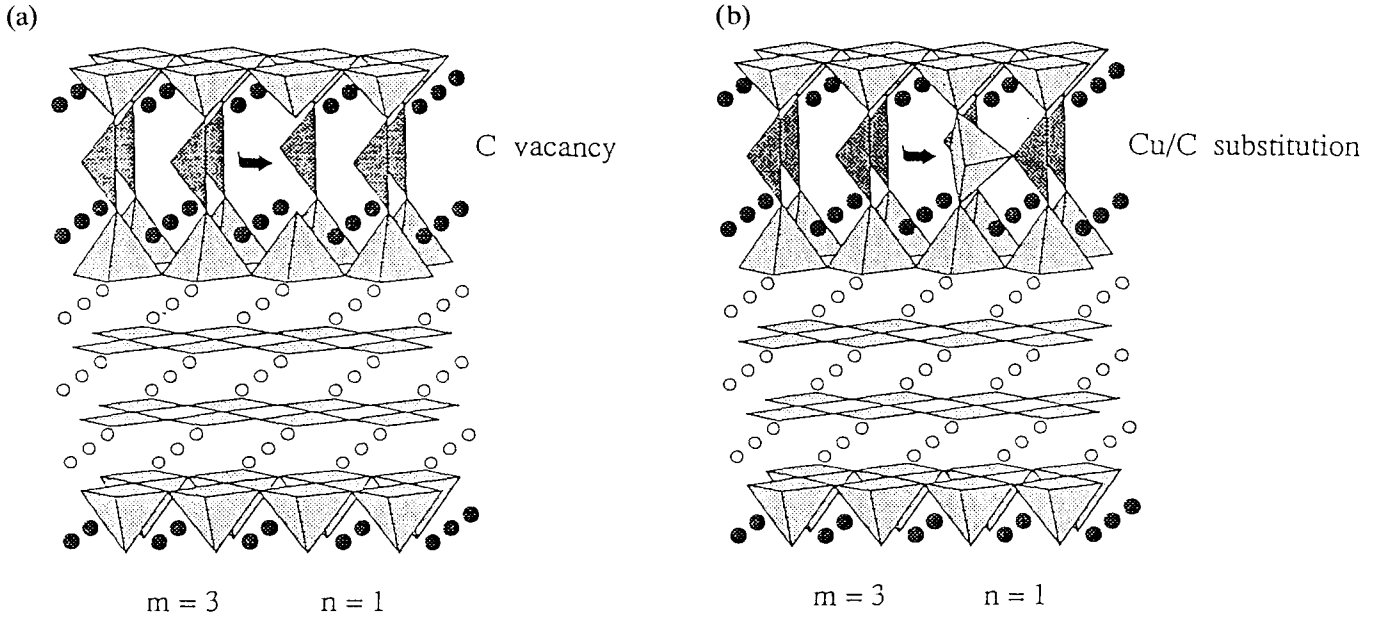


Fig. 14. Idealized structural models illustrating (a) the existence of carbonate group vacancies and (b) the partial replacement of carbonate groups by copper polyhedra; both events would statistically occur in the carbonate layers.

[13] C. Michel, M. Hervieu, M.M. Borel, A. Grandin, F. Deslandes, J. Provost and B. Raveau, *Z. Phys. B, 68* (1987) 421.
[14] M. Hervieu, M.T. Caldès, D. Pelloquin, C. Michel, S. Cabrera and B. Raveau, *J. Solid State Chem.*, submitted for publication.
[15] M. Huvé, C. Michel, A. Maignan, M. Hervieu, C. Martin and B. Raveau, *Physica C, 205* (1993) 219.
[16] A. Maignan, M. Huvé, C. Michel, M. Hervieu, C. Martin and B. Raveau, *Physica C, 208* (1993) 149.
[17] C. Martin, D. Bougault, C. Michel, J. Provost, M. Hervieu and B. Raveau, *Eur. J. Solid State Inorg. Chem., 26* (1989) 1.
[18] M.H. Pan and M. Greenblatt, *Physica C, 176* (1991) 80.
[19] M.H. Pan and M. Greenblatt, *Physica C, 184* (1991) 235.
[20] F. Goutenoire, M. Hervieu, A. Maignan, C. Michel, C. Martin and B. Raveau, *Physica C, 210* (1993) 3, 4, 359.
[21] A.K. Ganguli and M.A. Subramanian, *J. Solid State Chem., 93* (1991) 250.
[22] H.C. Ku, M.F. Tai, J.B. Shi, M.J. Shich, S.W. Hsu, G.H. Hwang, D.G. Ling, T.J. Watson-Yang and T.Y. Lin, *Jpn. J. Appl. Phys., 28* (6) (1989) 923.
[23] I.K. Gopalakrishnan, J.V. Yakhmi and R.M. Iyer, *Physica C, 175* (1991) 183.
[24] S.N. Putilin, E.V. Antipov, O. Chmaissen and M. Marezio, *Nature, 362* (1993) 226.
[25] M. Vehara, S. Sahoda, H. Nakata, J. Akimitsu and Y. Matsui, *Physica C, 222* (1994) 27.
[26] C. Martin, M. Hervieu, M. Huvé, C. Michel, A. Maignan, G. Van Tendeloo and B. Raveau, *Physica C, 222* (1994) 19.
[27] D. Pelloquin, M. Hervieu, C. Michel, A. Maignan and B. Raveau, *Physica C, 227* (1994) 215.
[28] J.L. Allen, B. Mercey, W. Prellier, J.F. Hamet, M. Hervieu and B. Raveau, *Physica C, 241* (1995) 158.
[29] T. Kawashima, Y. Matsui and E. Takayama-Muromachi, *Physica C, 224* (1994) 69.
[30] M.A. Alario-Franco, P. Bordet, J.J. Capponi, C. Chaillout, J. Chevanas, T. Fournier, M. Mareizio, B. Souletie, A. Sulpice, J.-L. Tholence, C. Colliex, R. Argoud, J.L. Baldonedo, M.F. Gorius and M. Perroux, *Physica C, 231* (1994) 103.